

**A CFD SIMULATION STUDY ON THE EFFECT OF
VOLUME RATIO ON PRESSURE PILING**

DHIVYA LAKSHMI A/P MOHANA SUNDRAM

**BACHELOR OF CHEMICAL ENGINEERING (GAS TECHNOLOGY)
UNIVERSITI MALAYSIA PAHANG**

© DHIVYA LAKSHMI (2014)

Thesis Access Form

No _____ Location _____

Author :

Title :

Status of access OPEN / RESTRICTED / CONFIDENTIAL

Moratorium period: _____ years, ending _____ / _____ 20 _____

Conditions of access proved by (CAPITALS): SITI NORAISHAH BINTI ISMAIL

Supervisor (Signature).....

Faculty:

Author's Declaration: *I agree the following conditions:*

OPEN access work shall be made available (in the University and externally) and reproduced as necessary at the discretion of the University Librarian or Head of Department. It may also be copied by the British Library in microfilm or other form for supply to requesting libraries or individuals, subject to an indication of intended use for non-publishing purposes in the following form, placed on the copy and on any covering document or label.

The statement itself shall apply to ALL copies:

This copy has been supplied on the understanding that it is copyright material and that no quotation from the thesis may be published without proper acknowledgement.

Restricted/confidential work: All access and any photocopying shall be strictly subject to written permission from the University Head of Department and any external sponsor, if any.

Author's signature.....Date:

users declaration: for signature during any Moratorium period (Not Open work):

I undertake to uphold the above conditions:

Date	Name (CAPITALS)	Signature	Address

A CFD SIMULATION STUDY ON THE EFFECT OF VOLUME RATIO ON PRESSURE PILING

DHIVYA LAKSHMI A/P MOHANA SUNDRAM

Thesis submitted in partial fulfilment of the requirements
for the award of the degree of
Bachelor of Chemical Engineering (Gas Technology)

**Faculty of Chemical & Natural Resources Engineering
UNIVERSITI MALAYSIA PAHANG**

JANUARY 2014

© DHIVYA LAKSHMI (2014)

SUPERVISOR'S DECLARATION

We hereby declare that we have checked this thesis and in our opinion, this thesis is adequate in terms of scope and quality for the award of the degree of Bachelor of Chemical Engineering (Gas Technology).

Signature :
Name of main supervisor : SITI NORAISHAH BINTI ISMAIL
Position : LECTURER
Date : 23 JANUARY 2014

STUDENT'S DECLARATION

I hereby declare that the work in this thesis is my own except for quotations and summaries which have been duly acknowledged. The thesis has not been accepted for any degree and is not concurrently submitted for award of other degree.

Signature :
Name : DHIVYA LAKSHMI
ID Number : KC10010
Date : JANUARY 2014

Dedication

To my family, friends and lecturers

ACKNOWLEDGEMENT

I would like to thanks the following people and organisations;

- My supervisors Miss Siti Noraishah for her guidance through an effective well-arranged weekly meeting.
- Dr Jolius Gimbun for his guidance on Computational Fluid Dynamics (CFD) software.
- University Malaysia Pahang for providing me facilities to do this project.

ABSTRACT

This paper presents the CFD simulation study on the effect of volume ratio on pressure piling. The explosion of flammable mixtures in interconnected compartments is commonly defined as “pressure piling” and its occurrence is a relevant issue of industrial safety. Pressure piling is a situation where peak pressures much higher than the expected values predicted by thermodynamic are generated in the geometry. The geometric characteristics of the vessels such as the tube area and ratio of volumes of the interconnected vessels play important role in the intensity of the pressure piling. Moreover, pre-compression and violence of explosion are the two main mechanisms affecting pressure piling. A CFD-Ansys and RANS model were used in this paper. The models duplicated experimental explosion behaviours and the results were compared with experimental. Propane-air mixture was used to study pressure piling. In the end it was found that pre-compression and violence of explosion are the two main mechanisms affecting pressure piling, which in turns affect the ratio between reaction and venting time in the second vessel (Brt). Higher the Brt number in the second vessel, lower the occurrence of pressure piling. Lower the volume ratio, higher the violence of explosion. Increasing the volume ratio results in a more intense pre-compression (pressure in the secondary vessel at ignition time increases) thus suggesting that ignition in the second vessel occurs starting from a higher value of pressure. Therefore, low pre-compression and high Brt number can prevent the occurrence of pressure piling.

Key words: computational fluid dynamics, pressure piling, pre-compression, violence of explosion, volume ratio

TABLE OF CONTENTS

SUPERVISOR’S DECLARATION	IV
STUDENT’S DECLARATION	V
<i>Dedication</i>	VI
ACKNOWLEDGEMENT	VII
ABSTRACT.....	VIII
LIST OF FIGURES	X
LIST OF TABLES	XI
LIST OF ABBREVIATIONS.....	XII
LIST OF ABBREVIATIONS.....	XIII
1 INTRODUCTION	1
1.1 Motivation and statement of problem	1
1.2 Objectives.....	2
1.3 Scope of this research.....	2
1.4 Main contribution of this work	3
1.5 Organisation of this thesis	3
2 LITERATURE REVIEW	4
2.1 Overview	4
2.2 Pressure piling.....	4
2.3 Effect of volume ratio	7
2.4 Effect of interconnecting tube diameter and length	7
2.5 Pre-compression.....	10
2.6 Violence of explosion	11
2.7 Turbulent Bradley number Brt	13
2.8 Summary	14
3 METHODOLOGY	15
3.1 Overview	15
3.2 Simulation model and parameters	15
3.3 RANS Model.....	18
3.3.1 <i>Turbulent kinetic energy k</i>	18
3.3.2 <i>Rate of dissipation of turbulent kinetic energy ϵ</i>	19
3.3.3 <i>The standard k-ϵ model equations</i>	19
(3.9).....	19
3.4 Flowchart.....	20
3.5 Summary	20
4 RESULTS AND DISCUSSION.....	21
4.1 Overview	21
4.2 Results.....	21
4.3 Discussion	23
4.3.1 <i>Pre-compression</i>	23
4.3.2 <i>Violence of explosion</i>	24
4.3.3 <i>Coupling between pre-compression and violence of explosion</i>	26
5 CONCLUSION.....	28
5.1 Conclusion.....	28
5.2 Recommendations	28
REFERENCES	29

LIST OF FIGURES

Figure 2-1: Typical pressure curves from a pressure piling situation. Pressure in the secondary chamber (red) raises steadily until the flame arrives and a very fast combustion occur. At the point where the curves intersect flow direction through the opening is reversed (Rogstadkjernet, 2004).	6
Figure 2-2: Particle distributions at 50 ms for duct height and width: (a) 0.15m and 5 m, (b) 0.5m and 5m, (c) 0.15m and 15 m and (d) 0.5m and 15 m respectively (Kosinski and Hoffmann, 2006).	9
Figure 2-3: Typical waveform showing explosion pressure with oscillation (Marinovic, 1990).	11
Figure 2-4: Typical waveform showing pressure piling during explosion pressure rise ((Marinovic, 1990).	11
Figure 2-5: Comparison of correlation results for vent sizing and experiments for stoichiometric of methane-air mixture (A) and stoichiometric of propane-air mixture (B) (Di Benedetto, Salzano and Russo, 2005)	14
Figure 3-1: Simulation model (units are in cm).....	15
Figure 3-2: Volume ratio 8 meshed drawing in Gambit	16
Figure 3-3: Volume ratio 14 meshed drawing in Gambit	16
Figure 3-4: Volume ratio 22 meshed drawing in Gambit	17
Figure 3-5: Value of adjustable parameters of k-epsilon model.....	20
Figure 3-6: Simulation study procedures.....	20
Figure 4-1: Graph of P1 versus volume ratio	21
Figure 4-2: Graph of Pk versus volume ratio	22
Figure 4-3: Graph of P1 versus volume ratio	23
Figure 4-4: Velocity vector of mass flux from primary to secondary vessel for VR 14	24
Figure 4-5: Graph of turbulent intensity versus volume ratio	25
Figure 4-6: Graph of Pk versus volume ratio	26
Figure 4-7: Graph of pressure versus time step for VR14.....	27

LIST OF TABLES

Table 3-1: Four different volume ratios.....	15
Table 3-2: k-epsilon model constants for equations (3.9) and (3.10).....	16
Table 4-1: Pre-compression as function of volume ratio.....	23
Table 4-2: Turbulence intensity as function of volume ratio.....	24
Table 4-3: Peak pressure as function of volume ratio	26

LIST OF ABBREVIATIONS

C_1 constant of eq.(3.10)

c_1 constant of eq.(3.10)

c_2 constant of eq.(3.10)

Greek

k turbulent kinetic energy

ε rate of dissipation of turbulent kinetic energy

LIST OF ABBREVIATIONS

CFD	Computational Fluid Dynamics
VR	volume ratio
P1	pre-compression
Pk	peak pressure

1 INTRODUCTION

1.1 Motivation and statement of problem

In industry it is very common to find linked vessel configuration, such as interconnected reactors and tanks, mines, electrical equipment casings, adjacent buildings and so on. A problem which is quite often met, with interconnected tanks, or particularly, with furnaces, is that there are several interconnected vessels (Taylor, 1994). Di Benedetto and Salzano (2010) mentioned that the explosion of flammable mixtures in interconnected compartments is commonly defined as “pressure piling” and its occurrence is a relevant issue of industrial safety. Pressure piling is a situation where peak pressures much higher than the expected values predicted by thermodynamic are generated in the geometry. It was found from previous works that the geometric characteristics of the vessels play important role in the intensity of the pressure piling. Abdullin, Babkin, & Senachin, (1988); Di Benedetto & Salzano (2010); Lunn, Holbrow, Andrews, & Gummer, (1996); Maremonti, Russo, Salzano, & Tufano (1999); Rogstadkjernet, (2004); and Singh, (1977, 1994) proposed in their findings that tube area and ratio of volumes of the interconnected vessels effect the intensity of pressure piling rather than the length of interconnection tube. Moreover, according to Di Benedetto & Salzano (2010), pre-compression and violence of explosion are the two main mechanisms affecting pressure piling.

Estimating pressure loads from explosions is central in risk assessments (Di Benedetto & Salzano 2010). Prediction of an explosion can be a complex task since explosive combustion is intrinsically unsteady and strongly influenced by the feedback arising between flame, flow-field and geometry.

Therefore, Abdullin et al. (1988) and Singh (1994) proposed semi-empirical mathematical models (lumped parameter) to study the phenomenon. The interaction between the flame and the turbulent flow-field is described using empirical parameters like the turbulisation factor (X) in these models. Unfortunately, their applicability is mainly limited to the experimental conditions in which they are validated. Therefore, simulation of the unsteady interaction of flame propagation and geometry is needed to describe the phenomenon. To this aim, alternative approaches are based on the solution

of the Naviere-Stokes equations, coupled to the conservation equations for mass and energy (Di Benedetto & Salzano 2010). But the disadvantages are it is impossible to directly solve the Naviere-Stokes equations (DNS) and the use of Large Eddy Simulations (LES) technique is not practically applicable when it involves medium or large scale equipment. This is due to the fact that the computational resources are expensive. Therefore, Reynolds Averaged Naviere-Stokes (RANS) equations are used to perform simulations in most industrial applications. But in order for the RANS-based CFD model to duplicate the explosion phenomenon, it needs the aid of sub-models used for turbulence and combustion. Most of the commercial CFD codes are based on simplified laminar combustion model and on the derivation of the well-known EBU model (Spalding, 1977) or Eddy-Dissipation Model (Magnussen & Hjertager, 1977) for describing turbulent combustion. Health and Safety Laboratory (2002) and Mercx (1997) mentioned that these codes are mainly keen to the simulation of the interaction between obstacles and flame propagation targeting at conservatively approximating the pressure peak reached in equipment or large installation, e.g. offshores However, they still contain few empirical coefficients which have to be tuned in order to give reasonable results (Popat et al., 1996). A first attempt is made by Maremonti et al. (1999) at examining the capability of a CFD code, AutoReaGas to model gas explosions in interconnected vessels. The code was computer-generated the observed phenomenon by adjusting some parameters in the combustion model to duplicate the experimental behavior.

Here, a CFD-Ansys was used. The modal used was RANS. A stoichiometric mixture of propane-air was used.

1.2 Objectives

The following are the objectives of this research:

- To study the effect of volume ratio on pressure piling.

1.3 Scope of this research

The following are the scope of this research:

- i) A CFD-Ansys and RANS model were used to duplicate experimental explosion.

- ii) 8, 14 and 22 were the volume ratios used to study the effect of it on peak pressure.
- iii) The role played by pre-compression and violence of explosion on pressure piling were studied.

1.4 Main contribution of this work

This work contributes the way volume ratio effects pressure piling. How does a volume ratio can affect the peak pressure was analysed by studying the roles played by pre-compression and violence of explosion on pressure piling. Therefore, in order to do so three different volume ratios were used together with a stoichiometric propane-air mixture. A CFD-Ansys and RANS model were used to duplicate the experimental explosion and the simulation results were compared with experiment results.

1.5 Organisation of this thesis

The structure of the reminder of the thesis is outlined as follow:

Chapter 1 describes about the background, motivation and problem statement of the study. In the motivation, types of CFD techniques that are being used are discussed. Besides, objective and scopes are also being covered here.

Chapter 2 started off with the definition of pressure piling. The effect of volume ratio on pressure piling is being discussed also. They are based on previous studies done by several researchers. Moreover, the roles played by violence of explosion and pre-compression on pressure piling are discussed in this chapter too.

Chapter 3 is about the simulation model and parameters which were used in this study. The equations which are involved in this study are mentioned here.

Chapter 4 is the results and discussion section. This section elaborates about the findings in this simulation study. The comparisons between experiment and simulation results are elaborated here.

Chapter 5 is about the conclusion and recommendations where the conclusion of this study and the recommendations for better future studies has been mentioned here.

2 LITERATURE REVIEW

2.1 Overview

This paper presents the simulation studies on the effect of volume ratio on pressure piling. Pressure piling is defined as the high pressure generation in interconnected vessels when there is an explosion. When ignition occurs in a vessel, the explosion induced in the linked vessel can generate peak pressure much higher than the thermodynamic values based on the initial conditions. The explosion of gaseous flammable mixtures in linked vessels is recognised as a major source of risk in reactors and tanks in industry, mines, buildings, tankers, electrical equipment casings. In fact, such explosions show an anomalous destructive power deriving from rates of pressure rise and peak pressures much higher than those corresponding to explosions in single closed vessels (Bartknecht, 1981; Phylaktou & Andrews, 1993). It was found from previous works that the geometric characteristics of the vessels such as the tube area and ratio of volumes of the interconnected vessels play important role in the intensity of the pressure piling. Moreover, pre-compression and violence of explosion are the two main mechanisms affecting pressure piling.

2.2 Pressure piling

Many authors define pressure piling as a situation where peak pressures much higher than the expected values predicted by thermodynamic are generated in the geometry when there is an explosion. Australian Standard AS 2380.2-1991 defines pressure piling as “a condition resulting from ignition of pre-compressed gases in compartments or subdivisions other than those in which ignition were initiated (Bryers, n.d.). It also adds that pressure piling may occur “where an enclosure comprises two or more communicating compartments or is subdivided by the disposition of the internal parts of equipment. This generally results in an abnormally rapid rise of pressure and may lead to higher a higher maximum pressure that would otherwise be expected. The shape of the inside of the enclosure shall be such that pressure piling is precluded, as far as practicable. If it is impracticable to avoid the occurrence of pressure piling then the mechanical strength of the enclosure shall be increased to allow for it”. Therefore, the usual protective methods used in industry are explosion suppression and explosion relief venting. But, there is a third method which is being used is to build plant with enough

strength to contain the explosion and to prevent entirely the escape of any material even when the explosion is allowed to run its full course. The application of containment is being used when explosion of toxic materials are involved. But, the knowledge of application depends on the maximum pressure being generated by the explosion. According to Lunn et al. (1996) the maximum pressures in single vessel are usually in the range 7-10 times the operating pressure depending on the process conditions. Therefore, the vessel is then design to withstand the maximum explosion pressure, which can be measured in standard tests without rupture. Due to insensitivity to vessel size, the explosion peak pressure that a single vessel must withstand can be estimated directly from the small-scale tests maximum pressure.

When combustion is initiated inside a closed vessel, a finite amount of energy is released and the system will at any time be defined by the equation of state. In closed vessel combustion wave propagation is attended by a rise in pressure and mass flow which is first directed away from and later toward the point of ignition. As the flame travels outward from the ignition point, the temperature and pressure rises in the unburned gas in accordance with the law of adiabatic compression. As the flame travels outward from the point of ignition, the rate of combustion increases rapidly because of the increased flame area, the increased burning velocity and a relatively higher energy content in the unburnt gas caused by compression. In the initial phase the gas burns and expand at practically constant pressure and is subsequently compressed almost to its original volume as the last part of gas is consumed. In the vicinity of the orifice the gas movement is obviously much higher, and as the flame front approaches the orifice it will accelerate and at a certain distance tend to make a sudden transfer into the secondary chamber. When the flame eventually reaches the secondary chamber it will encounter a compressed turbulent mixture. Time between ignition and flame arrival in the secondary chamber, flow through the orifice and volume of the two chambers will decide what pre-ignition pressure will be at this time. As the jet shoot into the secondary chamber, a simultaneous ignition of a large area occurs. The high turbulence level will efficiently distribute radical species and heat, resulting in a very fast combustion process. Depending on combustion rate and the orifices ability to vent this secondary explosion, very high pressures can occur.

Byers (n.d) has done a case study about the explosion that has happened at North River No 1. Mine in Berry, Alabama on January 16, 1995. In his paper he discussed about the

generation of over pressures in flameproof enclosures when subjected to flammable gas explosions and the failure of a flameproof enclosure. He has concluded in his paper that the flameproof enclosure failed due to pressure piling and pressure wave superposition during methane explosion. He also has examined the mechanisms of overpressure generation during gas explosions in enclosures and the treatment of pressure piling in AS2380.2-1991.

Moreover, an occurrence of pressure piling in a flameproof motor which was being type tested by SIMTARS passed the dimensional requirements of AS2380.2, but when tested for flame containment it would consistently fail the flame transmission tests. It was found out that an internal fan at one end of the fan, which was used for cooling, could create conditions for pressure piling. Without the fan the motor consistently passed the same test it has previously failed and with fan reinstalled the motor could fail (Bryers, n.d.). Then, the fan was modified with slots to eliminate the pressure piling which had resulted, in this case in transmission of an internal ignition.

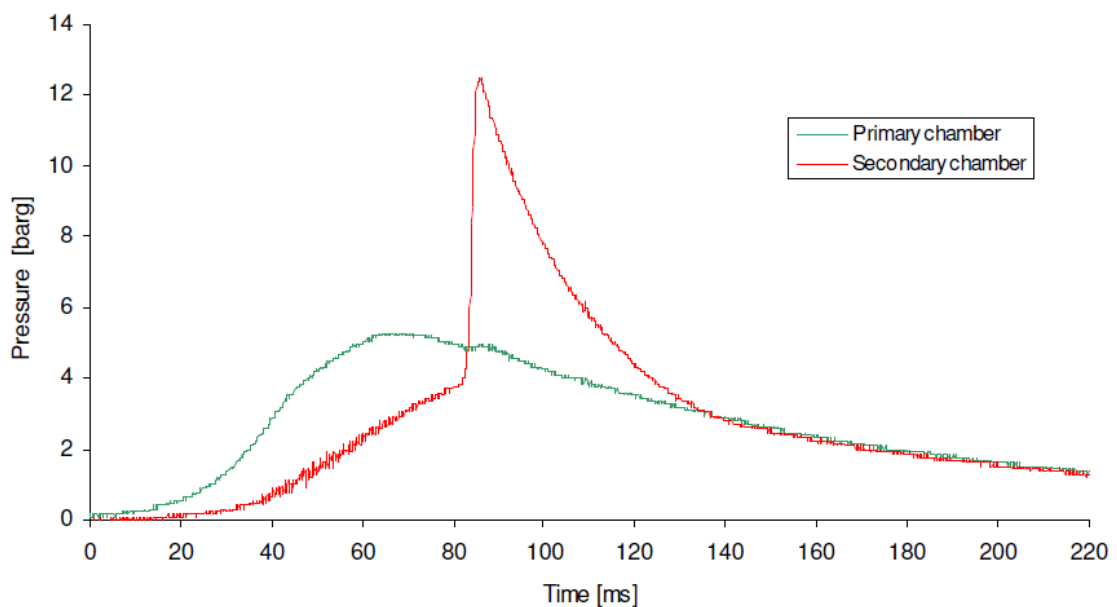


Figure 2-1: Typical pressure curves from a pressure piling situation. Pressure in the secondary chamber (red) raises steadily until the flame arrives and a very fast combustion occur. At the point where the curves intersect flow direction through the opening is reversed (Rogstadkjernet, 2004).

2.3 Effect of volume ratio

In the year of 1952, Gleim and Marcy examined effect of various volume ratios on the values of peak pressure. Their results showed higher peak pressures as volume ratio ($V_{\text{primary}}:V_{\text{secondary}}$) increased. Besides, Singh (1977, 1994) has done experiments on the importance of ignition location, volume ratio and size of transfer opening on maximum pressure and rate of pressure rise. He conducted experiments of similar setups but different scales. Through the experiments, he came to a decision that maximum pressure and rate of pressure rise was more obvious in larger scale setups. Although the conclusion may be right, the basis for it seems somewhat questionable since Singh did not change the size of the transfer opening. In the smallest setup the hole would therefore be relatively larger and hence result in a more efficient back venting of the secondary explosion ((Rogstadkjernet, 2004). Brown (1959) has also described the ratio of the volumes of the two vessels as an important factor in determining explosion pressures. He has stated in his paper that with a ratio of volumes at 13.5, the explosion pressure of 35 bar was measured.

On the other hand, Lunn, et al. (1996) reported about dust explosions with coal in enclosed interconnected vessels. In their experiment, they gave importance for volume ratio and diameter of transfer opening and found out there is no pressure piling occurred for volume ratios less than a quarter. When they conducted experiments in smaller-scale setup, it showed higher peak pressures and higher rate of pressure rise than a similar setup ten times the size. Therefore, in their report it was stated that for a given tube diameter, pressure piling effects are less noticeable in large-scale situations. But, this is something opposite to what Singh has said. The difference in scale between the two setups could be the reason behind it since Singh has used volume ratio ranging from 2 till 32, and connecting tube diameter ranging from 12-51mm, while Lunn, et al. have used several vessels with sizes ranging between 2 m^2 and 20 m^2 connected with 5m tubes of various diameters (15, 25, 50 cm).

2.4 Effect of interconnecting tube diameter and length

Many researches have done research on the effect of tube diameter on pressure piling in two interconnecting vessels. Kosinski and Hoffmann (2006) have done an investigation on the consequences of primary dust explosions in interconnecting vessels. They had used Eulerian-Lagrangian 2D computer simulations to describe the consequences of

primary dust explosions in two vessels connected by a duct. Since their objective was to model the system up to the time of ignition, thus they never consider any chemical reactions in the model. They analysed the phenomena responsible for the ignition of the dust in interconnected units by simulating the fluid flow and heat transfer. They performed the computation for different length and diameters of the interconnecting duct. In their simulation the length and the diameter of the duct had varied as 5 or 15 m and 0.15 and 0.5 m respectively. The investigation parameters were based on study done by Andrews and Lunn (2000) and the main conclusions too. The two main conclusions were the probability of ignition decreases with decreasing duct diameter and increases with decreasing duct length respectively. In the end, Kosinski and Hoffmann (2006) have concluded that the two main conclusions of Andrews and Lunn (2000) were same as theirs. For a bigger diameter of the duct the numbers of hot particles tend to increase. Meanwhile, the percentage of the hot particles is lower for longer tube. Moreover, they also have stated that when the particles form clusters with high concentration they create many “void regions”, thus it is not always possible to ignite a dust mixture in the secondary vessel. The large “void spaces” are the results of the tendency of the dust to locate in clouds with higher concentration. Turbulent flow in dust-air mixtures is likely to generate strong concentration gradients, thus giving rise to rich and lean zones. They may have considerable influence on the turbulent dust explosions propagation mechanisms.

The higher the duct diameter is the higher the area of void regions. Even if the initial uniform dust concentration is below the lower explosion limit, an ignition may still occur. This is due to fact that the dust particles may form clouds wherein concentration is above the explosion limit. This may be one of the reasons why it is more difficult to ignite the mixture in the secondary vessel for smaller diameters of the connecting ducts in experiments (Kosinski and Hoffmann, 2006). Figure 2-2 shows the particle distributions at 50 ms after the rupture of the “diaphragm” between the primary vessel and the duct for different duct diameters and length.

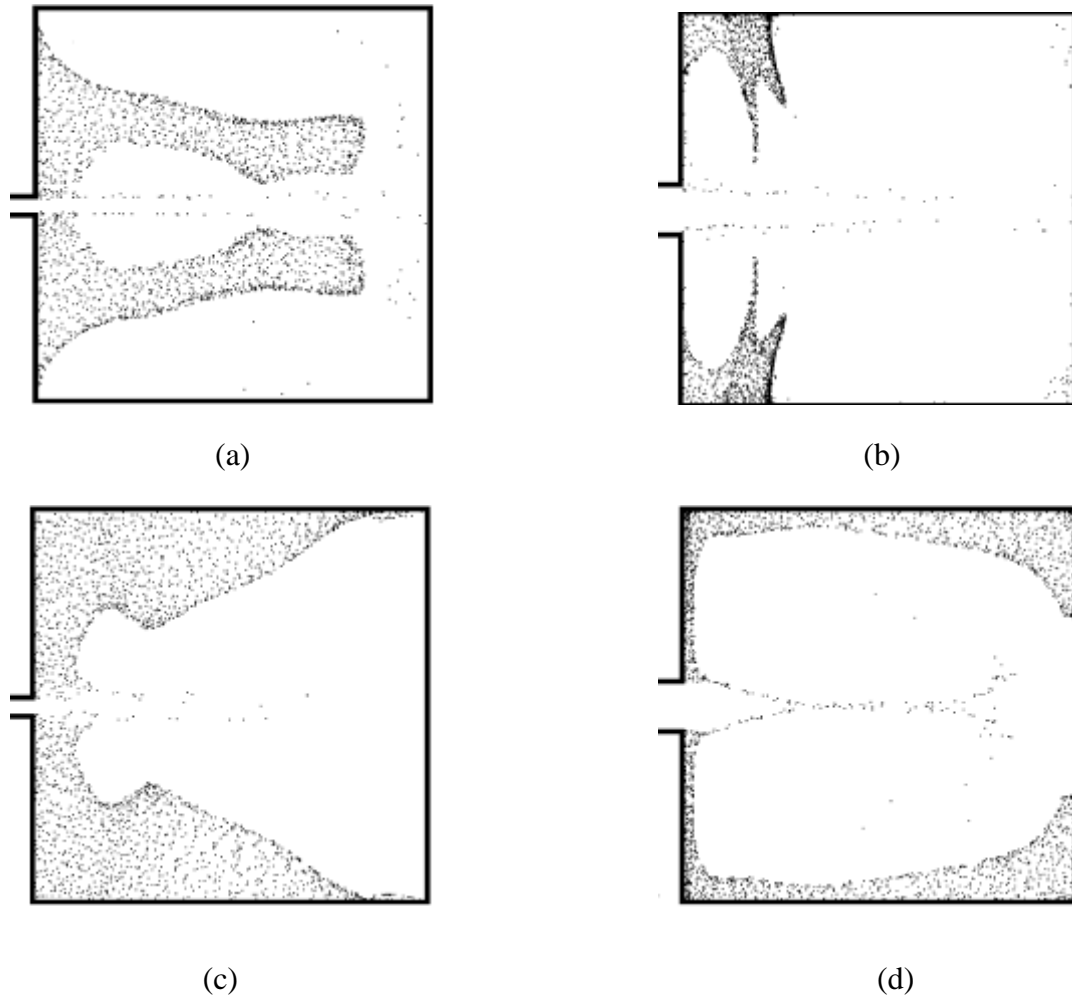


Figure 2-2: Particle distributions at 50 ms for duct height and width: (a) 0.15m and 5 m, (b) 0.5m and 5m, (c) 0.15m and 15 m and (d) 0.5m and 15 m respectively (Kosinski and Hoffmann, 2006).

Besides, the size of the connecting duct affects for the speed of the explosion. It was found that the process is the slowest for the longer tube with the smaller diameter where the mixing process is less intense and the temperature rise of the particles is moderate. Moreover, the size of the jet influences the probability of the explosion where the number of hot particles is increased and they are also pushed to form clouds with higher concentration thus leading to higher probability of an explosion.

However, there were few problems being encountered while running this investigation. One of them was the initial distribution of pressure where the pressure in the primary vessel after explosion was assumed to be uniform. But this is not true because after an ignition of a combustible mixture, a flow of gas from the vessel to the duct begins and this process continues during the explosion leading to a pressure drop in the primary vessel and a pressure rise in the duct and later in the secondary vessel.

2.5 Pre-compression

As stated earlier, violence of explosion and pre-compression are the two main mechanisms involved in pressure piling. When flame propagates in the primary vessel, pressure will increase and a flux of unburned gases from the primary vessel towards the secondary vessel happens while the flame is still in the primary vessel. This mass flux from the primary vessel towards the secondary causes an increase of pressure in the secondary vessel, which is known as pre-compression. Lunn et al. mentioned that pre-compression is caused by the venting of material from the primary explosion. Consequently, when the flame enters the second vessel, ignition occurs at an initial pressure which is higher than the atmospheric pressure (Di Benedetto and Salzano, 2010).

Marinovic (1990) has discussed about two types of overpressure generated in gas explosions. The first is an oscillatory pressure waveform that is superimposed on the envelope of the pressure rise and the second is the overpressures caused by pressure piling. He has mentioned that the pressure waveform is attributed to pressure wave reflections, and commonly found in irregularly shaped enclosures. The oscillations introduce dynamic stresses on an enclosure which can increase the combined stress on the enclosure by up to 5% in severe cases (Marinovic, 1990). Moreover, the amount of energy which can be released into the part of enclosure is affected by the density of the gas in that enclosure and it is directly related to the pressure rise generated when an ignition occurs. Hence, if a pressure wave causes unburnt gas to be compressed ahead of the wavefront, then when the pre-compressed gas ignites, it will generate an overpressure (Byers (n.d).

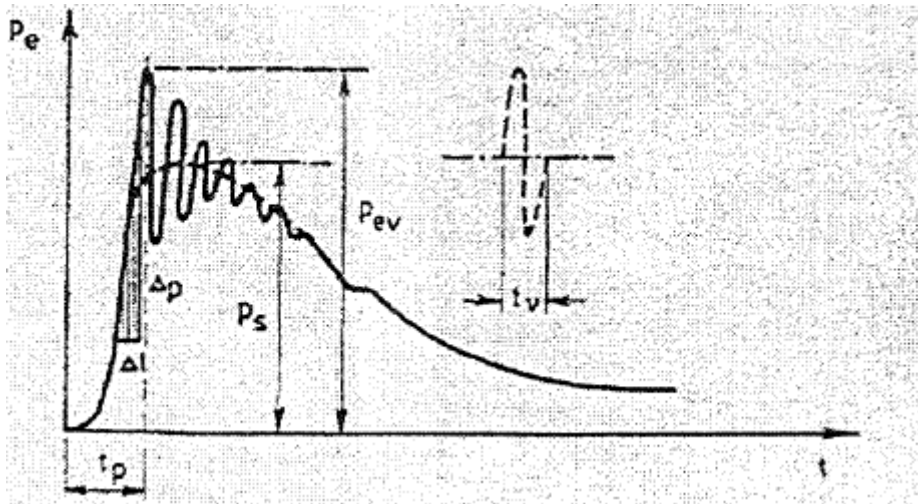


Figure 2-3: Typical waveform showing explosion pressure with oscillation (Marinovic, 1990).

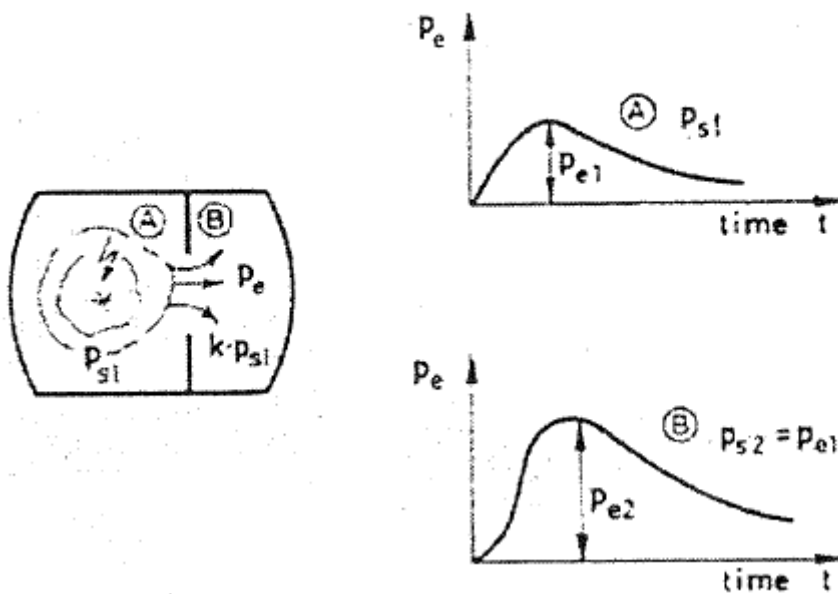


Figure 2-4: Typical waveform showing pressure piling during explosion pressure rise ((Marinovic, 1990).

2.6 Violence of explosion

Di Benedetto and Salzano (2010) proposed that the increase of initial pressure has a dramatic effect on the pressure peak as it is strongly coupled to the violence of explosion in the second vessel. Due to jet injection, two eddies will be formed near the entrance of secondary vessel, thus induce turbulence in the secondary vessel. The

generation of intense turbulence leads to an increase of the flame propagation velocity. Eventually, the peak pressure measured after the entry of flame in the secondary vessel can be much higher than adiabatic value evaluated thermodynamically from initial atmospheric conditions. This is the result of the balance in the second vessel between the rate of production of burnt gases (the turbulent combustion) and the mass flow (the venting) through the connecting duct towards the first vessel (Di Benedetto, Salzano and Russo, 2005).

Abdullin et al. (1988) and Phylaktou & Andrews (1993) have studied about the passage of the flame along the pipe. They say that when there is high flame speed in the pipe, the explosion flame entering the second vessel acts as a flame-jet ignition source of the turbulent and possibly pre-pressurized mixture. According to Maremonti et al. (1999) the induced turbulence in the secondary vessel is a major factor affecting the explosion violence. Eventhough the conditions under which this secondary explosion takes place are generally unknown, previous researches have proved that in some circumstances there can be a significant increase in the rate of combustion, violence of the explosion and explosion pressures. The reasons for this increase in the rate of combustion are the generation of turbulence as the explosion passes through the interconnecting pipe and the entry into the second vessel of a relatively large jet flame ignition source (Lunn et al., 1996). If the explosion is totally contained, then pressure piling may give pressures higher than expected on the basis of single-vessel results.

Bartknecht (1978) says in his results that for an enclosed system with equal volume of vessels that the peak pressure in the secondary vessel is higher than in a single vessel and the rate of pressure rise due to the explosion is markedly increased in both vessels, especially in secondary vessel. In his experiments, he stated that the violence of explosion is increased by a factor ranging from 3-10 and is measured by rate of pressure rise. Besides, Phylaktou and Andrews (1993) have measured the enhancements of the explosion violence in linked vessels in their experiments. They found that the violence of explosion in the secondary vessel was further increased when the primary ignition position was at the rear of the first vessel rather than at the centre. The interconnected vessels' volumes were 1 and 5 m³ in Bartknecht's experiment with methane-air explosions. He has also stated that the pressures and the rate of pressure rise depended on the vessel in which the primary ignition took place. The values of rate of pressure rise were similar in both vessels for ignition in smaller vessel eventhough the values

increased as the pipe diameter increased from 0.1 to 0.4 m. Besides, the peak pressure increases in both vessels as the pipe diameter increases with the peak pressure in the secondary vessel being less than in the primary at the lower pipe diameter.

In the experiments done by Singh (1994) at a fixed ratio of vessel volumes and connecting tube diameter, an increase in the primary chamber volume increased the peak pressure. This proves that the scale effect was dominant although the volume ratio between the vessels had an important effect on the pressure piling. The flow induced in the pipeline by the explosion in the primary ignition vessel increases turbulence in both the pipe and the secondary vessel. This is the reason for the greater violence. As Phylaktou and Andrews (1993) pointed out, the maximum rate of pressure rise is an important characteristic for determining the venting requirements of vessels. They have stated that high explosion violence in the secondary vessel may make venting of secondary vessel difficult, if not possible. Furthermore, they have also stated that backflow from the secondary vessel into the primary vessel can increase the violence of explosion the primary vessel.

2.7 Turbulent Bradley number Br_t

Molkov, Dobashi, Suzuki, and Hirano (2000) proposed a turbulent Bradley number (Br_t), the ratio of reaction time to venting time for turbulent flame propagation. Di Benedetto, Salzano and Russo (2005) have done research on predicting pressure piling by semi-empirical correlations. They modelled two interconnected vessels as two vented vessels and empirical correlations available for vent sizing were applied to reproduce the peak pressure reached in pressure piling. They had used NFPA, Yao, Bradley and Mitcheson and Molkov correlations. The comparison between those correlations is shown in Figure 2-4. In the end of study, they concluded that among those correlations the most suitable appears to be Molkov's which takes into account the effect of initial pressure and turbulent flame propagation. The validity of the correlation proves that pre-compression and the turbulent Bradley number are the major factor affecting pressure piling. Di Benedetto and Salzano (2010) stated that at low values of turbulence level i.e. very high Br_t numbers (Br_t approaches infinity), reaction time is much lower than the venting time and the peak pressure can be significantly lower than the thermodynamic value corresponding to the pressure in the secondary vessel at ignition time. Conversely, for very low Br_t number, the flame propagation is much

faster than venting. Molkov's correlation was developed for a simply vented vessel and the validity of the correlation suggest that it could be assumed that the pressure rise and the pressure peak are not affected by the presence of the rest of the equipment, such as the duct and the interconnected vessel. This means the second vessel effectively behaves as a simply vented vessel. Even if it vents towards a pressure variable vessel through a duct, the reaction being much faster than venting ($Brt < 1$) during flame propagation, the vessel behaves as isolated. Therefore, increasing the volume ratio results in a more intense pre-compression (pressure in the secondary vessel at ignition time increases) thus suggesting that ignition in the secondary vessel occurs starting from a higher value of pressure. Consequently, at a fixed level of turbulence, the peak pressure should be higher.

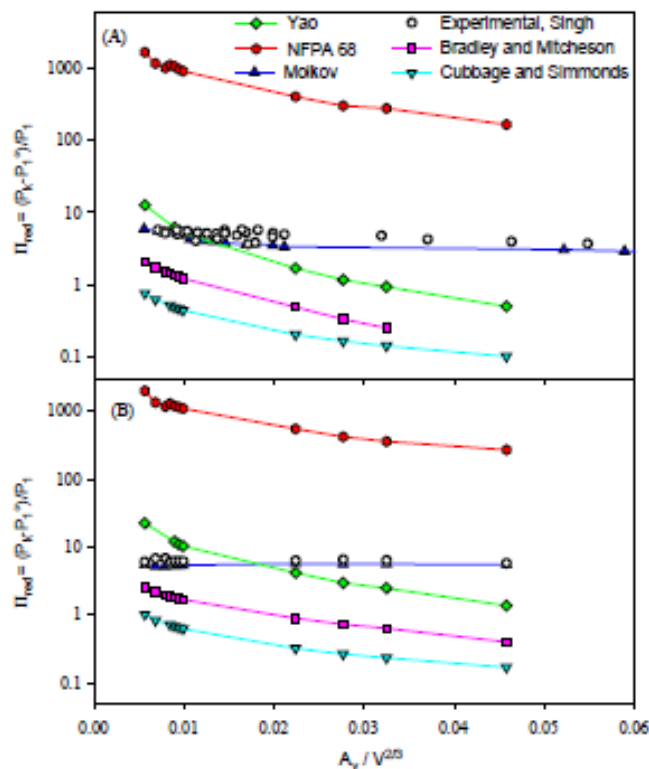


Figure 2-5: Comparison of correlation results for vent sizing and experiments for stoichiometric of methane-air mixture (A) and stoichiometric of propane-air mixture (B) (Di Benedetto, Salzano and Russo, 2005)

2.8 Summary

This chapter is all about previous studies related to pressure piling and their findings.

3 METHODOLOGY

3.1 Overview

Here, a CFD Ansys and RANS model were used to study the effect of volume ratio on pressure piling by duplicating experimental explosion. The simulation results were compared with experiment results. Three different volume ratios and propane-air mixture were used. The turbulence intensity, peak pressure and the pressure at the secondary vessel when the flame enters secondary vessel were determined too. All these values were then used to study the factors affecting pressure piling in two interconnected vessels. First, the geometry was drawn in Gambit. After it has been meshed, the meshed drawing was export to CFD Fluent to solve it.

3.2 Simulation model and parameters

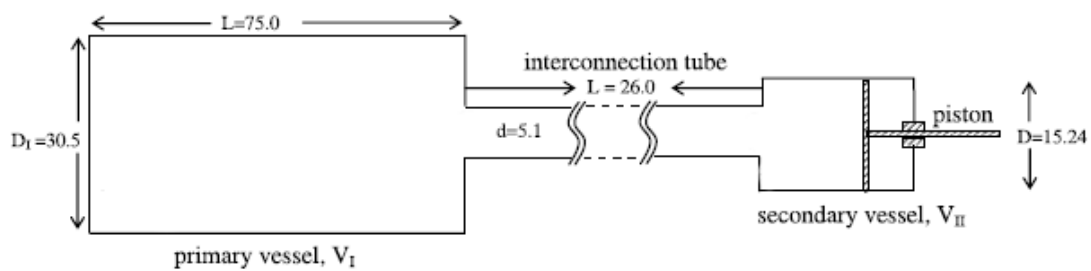


Figure 3-1: Simulation model (units are in cm)

Table 3-1: Four different volume ratios

Model	Primary Vessel Volume, V_I (m^3)	Volume Ratio, VR ($V_I:V_{II}$)	Secondary Vessel Volume, V_{II} (m^3)	Tube Length, L (m)	Tube Diameter, d (m)
1	5.46E-03	8	6.83E-03	0.26	0.051
2	5.46E-03	14	3.90E-03	0.26	0.051
3	5.46E-03	22	2.48E-03	0.26	0.051

Table 3-2: k-epsilon model constants for equations (3.9) and (3.10)

C _μ	0.09
C1-epsilon	1.44
C2-epsilon	1.92
TKE Prandtl Number	1
TDR Prandtl Number	1.3
Energy Prandtl Number	0.85
Energy Prandtl Number	0.85
Turbulence Schmidt Number	0.7

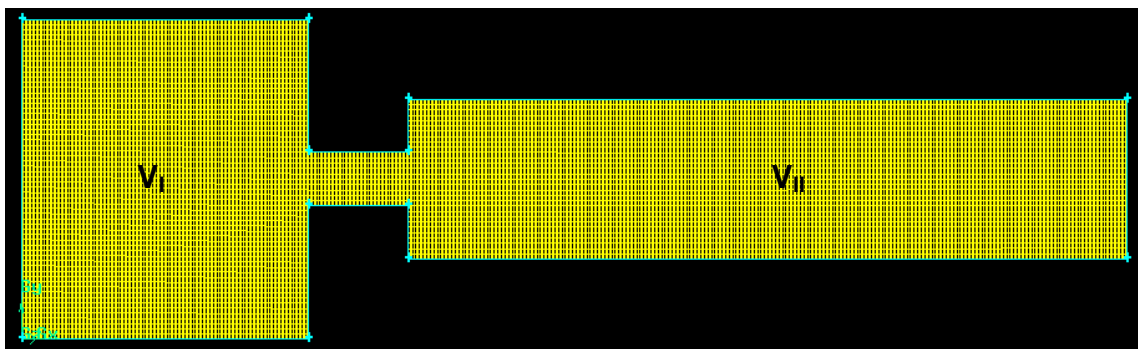


Figure 3-2: Volume ratio 8 meshed drawing in Gambit

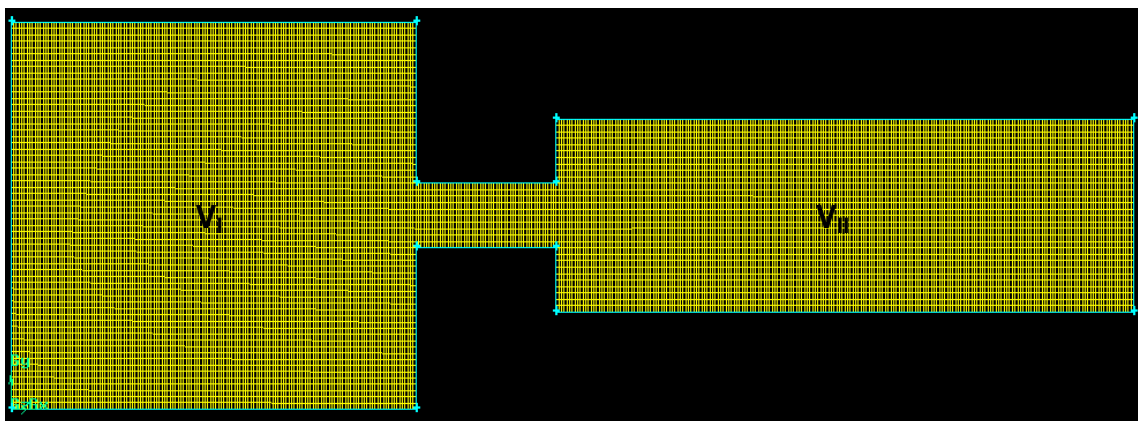


Figure 3-3: Volume ratio 14 meshed drawing in Gambit

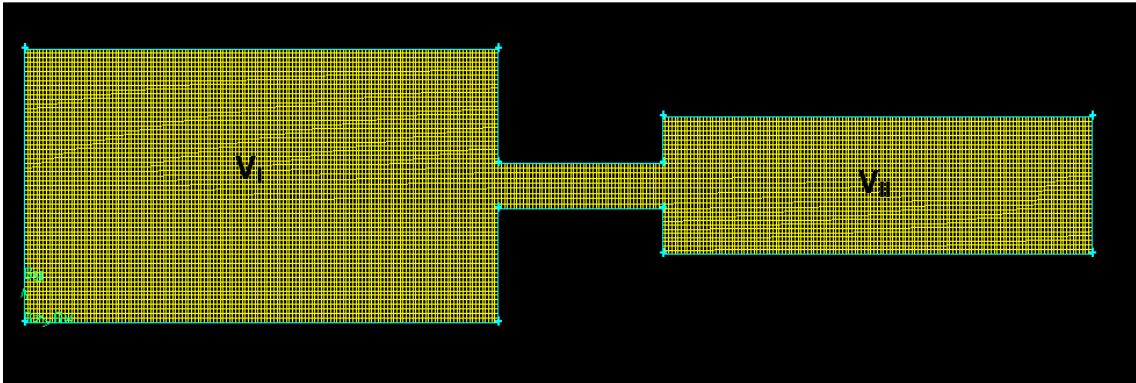


Figure 3-4: Volume ratio 22 meshed drawing in Gambit

According to Di Benedetto and Salzano (2010), the unsteady Reynolds average energy, momentum and mass balances equations which were used as follows:

Continuity equation

$$\frac{\partial \bar{\rho}}{\partial t} + \frac{\partial}{\partial x_j} (\bar{\rho} \tilde{u}_j) = 0 \quad (3.1)$$

Momentum balance equation:

$$\frac{\partial (\bar{\rho} \tilde{u}_i)}{\partial t} + \frac{\partial}{\partial x_j} (\bar{\rho} \tilde{u}_j \tilde{u}_i) = -\frac{\partial \bar{P}}{\partial x_i} - \frac{\partial}{\partial x_j} (\overline{\rho u_j'' u_i''}) \quad (3.2)$$

Energy balance equation:

$$\frac{\partial (\bar{\rho} \tilde{e})}{\partial t} + \frac{\partial}{\partial x_j} (\bar{\rho} \tilde{u}_j \tilde{e}) = -\bar{P} \frac{\partial \tilde{u}_j}{\partial x_j} - \frac{\partial}{\partial x_j} (\overline{\rho u_j'' e''}) \quad (3.3)$$

Progress variable equation:

$$\frac{\partial (\bar{\rho} \tilde{c})}{\partial t} + \frac{\partial}{\partial x_j} (\bar{\rho} \tilde{u}_j \tilde{c}) = -\bar{\omega} - \frac{\partial}{\partial x_j} (\overline{\rho u_j'' c''}) \quad (3.4)$$

Source: Journal of Loss Prevention in the Process Industries 23 (2010), 498-506

Where,

ρ = density

P = pressure

u = velocity

c = progress variable

e = internal energy

A commercial CFD solver (CFD-Ansys) was used for the numerical solution. The transient calculations were performed by means of the Cranke-Nicholson scheme. The Courant condition control for time-stepping was used for the evaluation of the maximum time step (Morton & Mayers, 1994):

$$\Delta t = CFL \frac{\Delta l}{|u| + c}$$

Where, CFL is the Courant number, c is the sound velocity, Δl is the dimension of the control volume and $|u|$ is the magnitude of the local velocity.

3.3 RANS Model

In this paper the Reynolds-averaged Navier-Stokes (RANS) equations were used to solve turbulence modeling. The laminar finite-rate was used to study turbulence-chemistry interaction. In order to be able to compute turbulent flows with the RANS equations it is necessary to develop turbulence models to predict the Reynolds stresses and the scalar transport terms and close the system of mean flow equations (Versteeg and Malalasekera, 2007). The RANS turbulence model used in this paper was the $k - \epsilon$ model. This model is a more sophisticated and general description of turbulence which allows for the effects of transport of turbulence properties by convection and diffusion and for production and destruction of turbulence. This $k - \epsilon$ model has two transport equations which are one is for the turbulent kinetic energy k and another one is for the rate of dissipation of turbulent kinetic energy ϵ . This $k - \epsilon$ or k-epsilon model focuses on the mechanisms that affect the turbulent kinetic energy. Below are the two transport equations for $k - \epsilon$ model.

3.3.1 Turbulent kinetic energy k

$$k(t) = K + k \tag{3.5}$$

Where K is mean kinetic energy and k is turbulent kinetic energy

Mean kinetic energy K

Rate of change of mean kinetic energy K + Transport of K by convection = Transport of K by pressure + Transport of K by viscous stresses + Transport of K by Reynolds stress - Rate of viscous dissipation of K - Rate of destruction of K due to turbulence production

$$\frac{\partial(\rho K)}{\partial t} + \text{div}(\rho K \mathbf{U}) = \text{div}(-P \mathbf{U} + 2\mu \mathbf{U} S_{ij} - \rho \mathbf{U} \overline{u'_i u'_j}) - 2\mu S_{ij} \cdot S_{ij} + \rho \overline{u'_i u'_j} \cdot S_{ij} \quad (3.6)$$

Turbulent kinetic energy k

Rate of change of turbulent kinetic energy k + Transport of k by convection = Transport of k by pressure + Transport of k by viscous stresses + Transport of k by Reynolds stress - Rate of dissipation of k + Rate of production of k

$$\frac{\partial(\rho k)}{\partial t} + \text{div}(\rho k \mathbf{U}) = \text{div}(-\overline{p' \mathbf{u}'} + 2\mu \overline{\mathbf{u}' s'_{ij}} - \rho \frac{1}{2} \overline{u'_i \cdot u'_i u'_j}) - 2\mu \overline{s'_{ij} \cdot s'_{ij}} - \rho \overline{u'_i u'_j} \cdot S_{ij} \quad (3.7)$$

3.3.2 Rate of dissipation of turbulent kinetic energy ε

$$\varepsilon = 2\nu \overline{s'_{ij} \cdot s'_{ij}} \quad (3.8)$$

3.3.3 The standard k - ε model equations

Rate of change of k or ε + Transport of k or ε by convection = Transport of k or ε by diffusion + Rate of production of k or ε - Rate of destruction of k or ε

$$\frac{\partial(\rho k)}{\partial t} + \text{div}(\rho k \mathbf{U}) = \text{div} \left[\frac{\mu_t}{\sigma_k} \text{grad } k \right] + 2\mu_t S_{ij} \cdot S_{ij} - \rho \varepsilon \quad (3.9)$$

$$\frac{\partial(\rho \varepsilon)}{\partial t} + \text{div}(\rho \varepsilon \mathbf{U}) = \text{div} \left[\frac{\mu_t}{\sigma_\varepsilon} \text{grad } \varepsilon \right] + C_{1\varepsilon} \frac{\varepsilon}{k} 2\mu_t S_{ij} \cdot S_{ij} - C_{2\varepsilon} \rho \frac{\varepsilon^2}{k} \quad (3.10)$$

(Source: An Introduction to Computational Fluid Dynamics, 2007)

Where the five adjustable parameters value are shown in Figure 3-5.

$$C_{\mu} = 0.09 \quad \sigma_k = 1.00 \quad \sigma_{\epsilon} = 1.30 \quad C_{1\epsilon} = 1.44 \quad C_{2\epsilon} = 1.92$$

Figure 3-5: Value of adjustable parameters of k-epsilon model.

3.4 Flowchart

The flowchart below shows the procedures of this simulation.

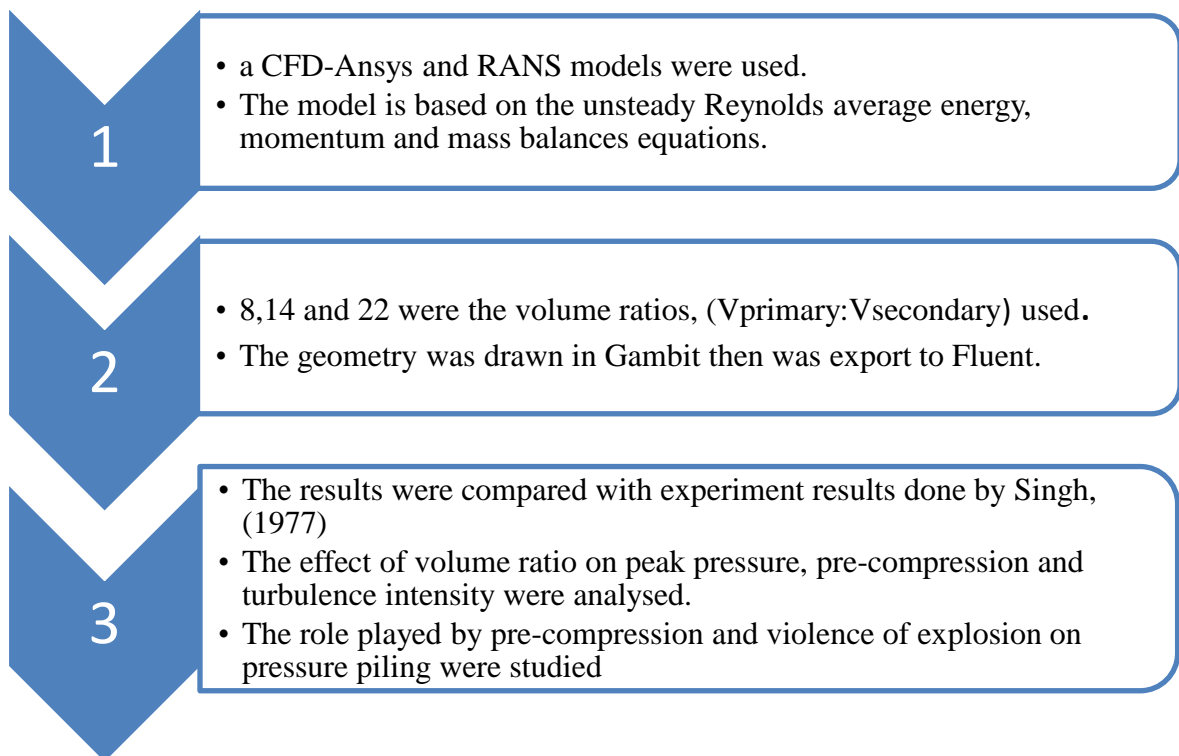


Figure 3-6: Simulation study procedures

3.5 Summary

This chapter describes about the modal and parameters together with the equations involved in this simulation study.

4 RESULTS AND DISCUSSION

4.1 Overview

This chapter describes about the findings from this simulation study. The results were compared with experimental results and the mechanisms affecting pressure piling were looked in details.

4.2 Results

The results from this study were compared with Singh (1977) experimental results. The peak pressure, P_k and the pre-compression, P_1 values gained in this simulation study were compared mainly with the experimental results. The compared values are shown in the Figure 4-1 and Figure 4-2 respectively.

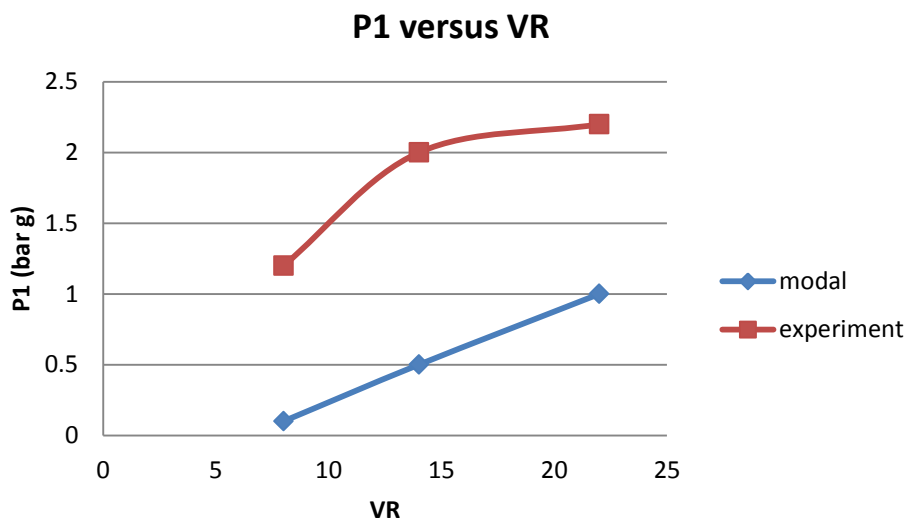


Figure 4-1: Graph of P_1 versus volume ratio

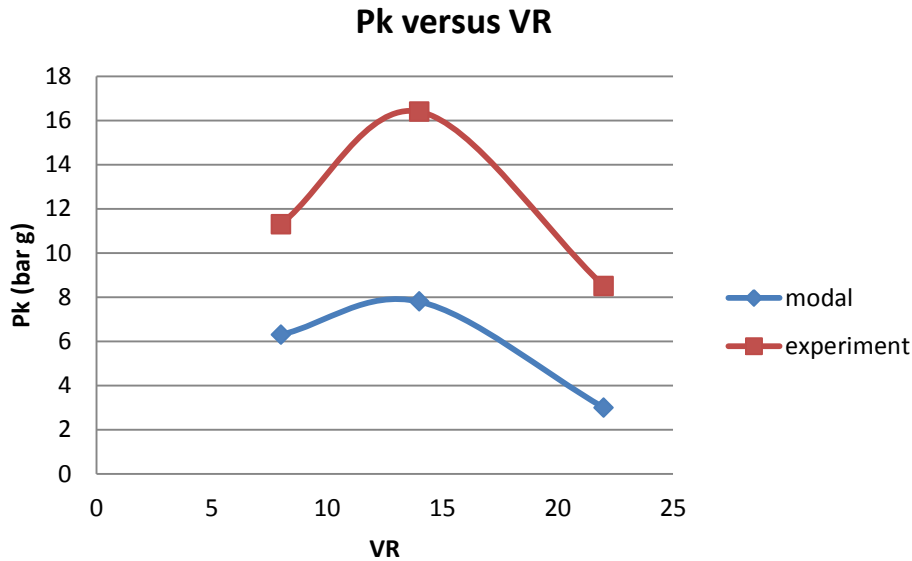


Figure 4-2: Graph of Pk versus volume ratio

From both the graphs it can be seen that the CFD model is unable to predict the experimental phenomenon. The error between the simulation and experiment results are 44.24%, 51.5% and 64.7% for volume ratio of 8, 14 and 22 respectively. Although there is deviation, but the trend of the results is the same as the experimental for both pre-compression and peak pressure case. The results in Figure 4-2 show linear relationship between volume ratio and pre-compression pressure. The CFD model is unable to predict the experimental phenomena exactly maybe due to the inability of the k-epsilon model to predict turbulence intensity correctly. Since peak pressure is related to turbulence intensity, therefore it gives results far from experiment. In this simulation study since the trend is similar to experimental phenomenon, thus the results will be used to study the mechanisms involved in producing pressure piling.

The k-epsilon model has five adjustable parameters. The production and destruction of turbulent kinetic energy are always closely linked. The dissipation rate ϵ is large when the production of k is large. The model equation (3.10) for ϵ assumes that its production and destruction terms are proportional to the production and destruction terms of the k -equation (3.9). This ensures that ϵ increases rapidly if k increases rapidly and that it decreases sufficiently fast to avoid (non-physical) negative values of turbulent kinetic energy if k decreases. Therefore, the factor ϵ/k in the production and destruction terms makes these terms dimensionally correct in the ϵ -equation. The constants $C_{1\epsilon}$ and $C_{2\epsilon}$ as

in Figure 3-5 are important to give correct proportionality between the terms in the k - and ε -equations.

4.3 Discussion

4.3.1 Pre-compression

Table 4-1: Pre-compression as function of volume ratio

Model	Primary Vessel Volume, V_I (m^3)	Volume Ratio, VR ($V_I:V_{II}$)	Secondary Vessel Volume, V_{II} (m^3)	Pre-compression, P_1 (bar g)
1	5.46E-03	8	6.83E-03	0.1
2	5.46E-03	14	3.90E-03	0.5
3	5.46E-03	22	2.48E-03	1.0

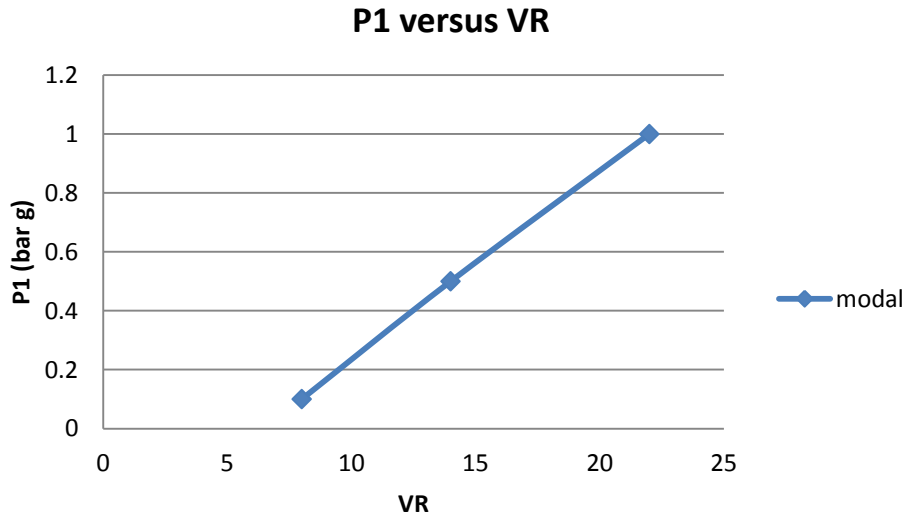


Figure 4-3: Graph of P1 versus volume ratio

The pressure at secondary vessel was observed in this study. From the results in Figure 4-3 it can be seen that the value of pre-compression increases as the volume ratio increases. It was found that when the flame enters the secondary vessel the pressure, P_1 at which the ignition happens is higher than initial pressure (1 atm). Throughout this experiment, the ignition position was defined at the centre of primary vessel ($x = 0.38\text{ m}$, $y = 0.15\text{ m}$) since centre ignition position is considered. The pressure starts to increase sharply after the flame enters the secondary vessel. As the volume ratio increases, the pre-compression pressure P_1 increases too.

When the flame propagates in the first vessel, mass flux of unburned gases from primary to secondary vessel causes pressure to increase in the secondary vessel. This pressure increase is known as pre-compression. Therefore, when the flame enters the secondary vessel the combustion starts at higher pressure than the initial. Figure 4-2 shows the velocity vector of mass flux from primary to secondary vessel for volume ratio 14. For this volume ratio, the pre-compressed pressure when the flame enters the secondary vessel is about 0.1 bar g.

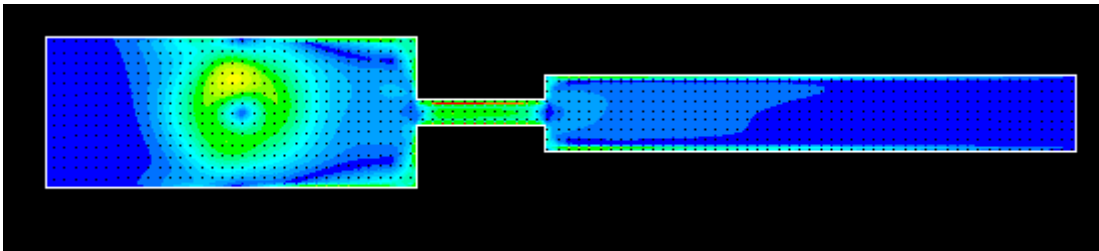


Figure 4-4: Velocity vector of mass flux from primary to secondary vessel for VR 14

This increase in pressure depends on the capacity of the receiver vessel, V_{II} . Higher volume ratio means lower secondary volume. Therefore, as the volume ratio increases the pre-compression pressure increases due to the lower capacity of the secondary volume to receive the venting materials from primary vessel. Thus the combustion in the secondary vessel starts at higher pressure too.

4.3.2 Violence of explosion

Table 4-2: Turbulence intensity as function of volume ratio

Model	Primary Vessel Volume, V_I (m ³)	Volume Ratio, VR ($V_I:V_{II}$)	Secondary Vessel Volume, V_{II} (m ³)	Turbulence intensity at secondary vessel
1	5.46E-03	8	6.83E-03	38
2	5.46E-03	14	3.90E-03	20
3	5.46E-03	22	2.48E-03	6

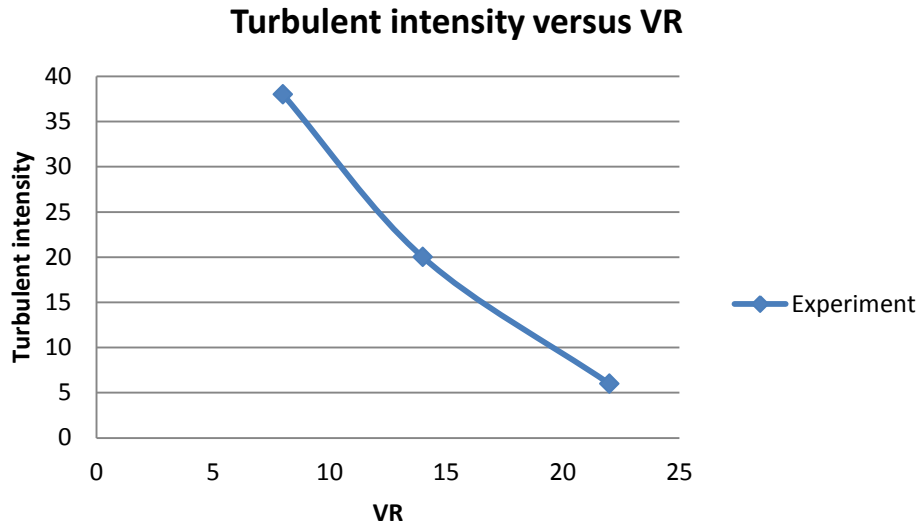


Figure 4-5: Graph of turbulent intensity versus volume ratio

The violence of explosion can be described in terms of turbulence intensity generated in the secondary vessel. From the results gained in this simulation study it can be seen that the turbulence intensity decreases as the volume ratio increases. Usually eddies will be formed at the entrance of secondary vessel when there is flux happens in the same vessel. This will create turbulence in the secondary vessel and steep pressure rise in the same vessel. Higher the turbulence intensity, higher the violence of explosion is expected to be and so the flame velocity.

According to Di Benedetto and Salzano (2010), the higher turbulence intensity is related to the intensity of jet injection caused by the pressure difference between primary and secondary vessels during flame propagation in the primary vessel. They also added that decreasing volume ratio leads to increasing pressure difference, which eventually increases the gas velocity in the interconnecting tube and in the secondary vessel. Therefore, higher secondary vessel volume gives higher turbulence intensity as the results gained in this simulation.

However, the effectiveness of venting through the interconnecting tube from the secondary to primary vessel need to be considered to study the influence on pressure piling. This is done by looking at the ratio between reaction time and venting time. This ratio is known as Bradley number and Molkov, et al., (2000) has proposed turbulent Bradley number (Br_t) for turbulent flame propagation. For high value of turbulence intensity, the turbulent Bradley number is lower. This means lower reaction time.

4.3.3 Coupling between pre-compression and violence of explosion

Table 4-3: Peak pressure as function of volume ratio

Model	Primary Vessel Volume, V_I (m^3)	Volume Ratio, VR ($V_I:V_{II}$)	Secondary Vessel Volume, V_{II} (m^3)	Peak pressure, P_k (bar g)
1	5.46E-03	8	6.83E-03	6.3
2	5.46E-03	14	3.90E-03	7.8
3	5.46E-03	22	2.48E-03	3.0

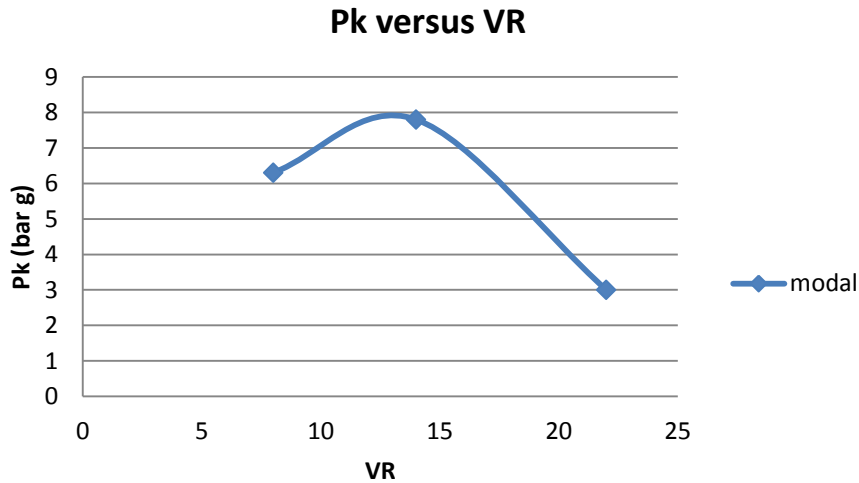


Figure 4-6: Graph of P_k versus volume ratio

As per discussed, the pre-compression pressure increases as the volume ratio increases. According to Figure 4-3, for the volume ratio of 14, the gained peak pressure is about 7.8 bar g at 50 ms. On the other hand, the turbulence intensity is higher as the volume ratio decreases. The high turbulence induced by the jet injection causes the reaction time to be very low, low Br_t . Therefore, there is no time for venting to take place. This is what had taken place for volume ratio of 8 and 14. The lower volume of secondary vessel has lead the pre-compression pressure to be higher, therefore the higher combustion initial pressure of secondary vessel has resulted in higher peak pressure.

On the other hand, lower value of turbulence intensity gives high value of Br_t as volume ratio 22. For higher turbulent Bradley number, the effectiveness of venting is higher although the reaction time is low. Due to the high effect of the venting, the high pre-compression pressure in the secondary vessel could not affect the peak pressure. Therefore, it can be concluded that peak pressure in interconnected vessel is due to the coupling between pre-compression and violence of explosion.

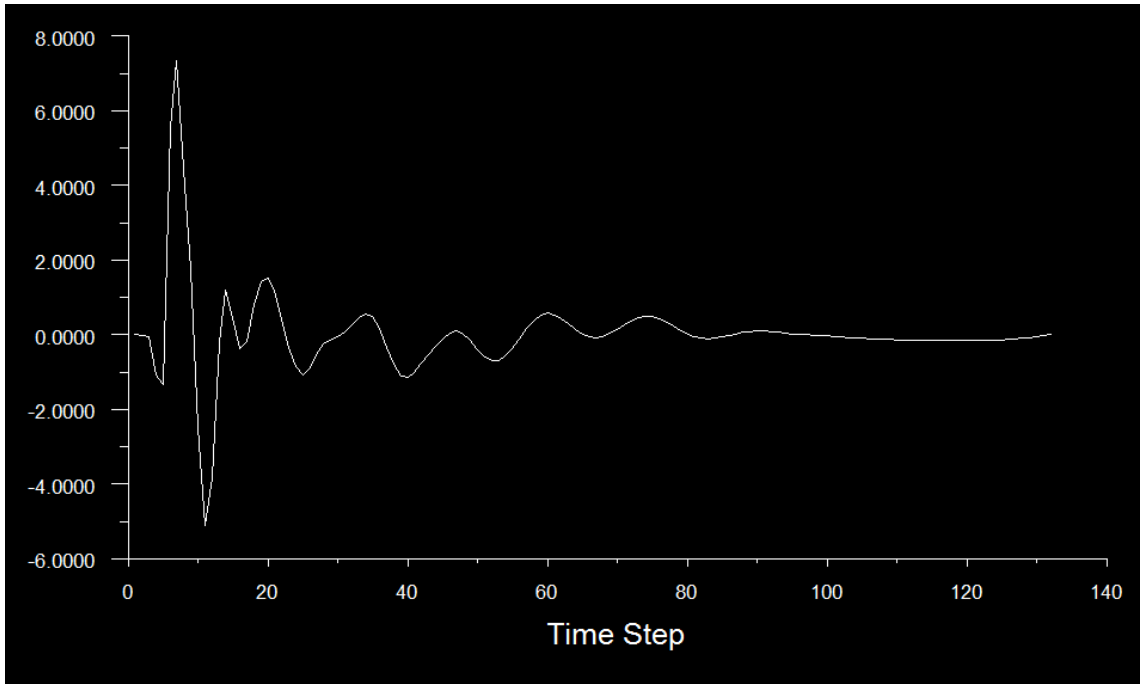


Figure 4-7: Graph of pressure versus time step for VR14

5 CONCLUSION

5.1 Conclusion

From the results it can be concluded that the pre-compression increases as volume ratio increases. Meanwhile, the turbulence intensity decreases as volume ratio increases. The highest peak pressure was found for volume ratio of 14 about 7.8 bar g. Pre-compression and violence of explosion are the two main mechanisms affecting pressure piling. Higher turbulent Bradley number and low pre-compression pressure could prevent explosions due to peak pressure. The CFD model is unable to reproduce the experimental phenomenon.

5.2 Recommendations

As a recommendation, maybe in order to reproduce satisfactory experimental phenomenon, three different types of combustion regime models like laminar, flamelet and distributed reaction zone combustion regimes could be used. For laminar combustion regime, the model is based on the flame propagation in the first vessel which is laminar in almost all its length. But close to the entrance of the tube, the turbulence is being enhanced due to the presence of the tube, thus wrinkling the flame. The flame starts to be distorted and combustion takes place as thin laminar flames which are stretched and convected by the turbulent motion eventhough their laminar flame structure is being retained. This regime is known as wrinkled flamelet regime. Two opposite effects will be observed when the flame enters secondary vessel. One is decrease of the flame propagation speed by the higher passage area and the other is increase of the flame speed due to the turbulence induced by jet ignition and injection. Therefore, due to these factors the combustion regime in the secondary vessel is known as a distributed reaction zone combustion regime. The advantage of these models is that the combustion models do not have adjustable parameters.

REFERENCES

- Abdullin, R. K., Babkin, V. S., & Senachin, P. K. (1988). Combustion of gas in connected vessels. *Combustion, Explosions and Shock Waves*, 24, 123-132.
- Abu-Orf, G. M., & Cant, R. S. (2000). A turbulent reaction rate model for premixed turbulent combustion in spark-ignition engines. *Combustion and Flame*, 122, 233-252.
- Andrews, S and Lunn, G.A. (2000). A report on some tests on the jet ignition of dust clouds, 2nd Internet Conference on Process Safety
- Australian Standard AS2380.2-1991 "Electrical equipment for explosive atmospheres- Explosion-protection techniques Part 2: Flameproof enclosure d", Standard Association of Australia, Sydney Australia.
- Bartknecht, W. (1981). *Explosion: Course, Prevention, Protection*. Berlin, Springer-Verlag.
- Bray, K. N. C., & Cant, R. S. (1991). *Proceedings of the Royal Society*, A434, 217.
- Bray, K. N. C., & Peters, N. (1994). Laminar flamelets in turbulent flames. In P. A. Libby, & F. A. Williams (Eds.), *Turbulence reacting flows*. London: Academic Press.
- Byers, K. J. (n.d.). Pressure piling and other issues affecting flameproof enclosures. Manager Engineering, Testing and Certification Centre.
- Di Benedetto, A. and Salzano, E. (2010). CFD simulation of pressure piling. *Journal of Loss Prevention in the Process Industries*, 23, 498-506.
- Di Benedetto, A., Salzano, E. and Russo, G. (2005). Predicting pressure piling by semi-empirical correlations. *Journal of Fire Safety*, 40, 282-298.
- Gleim, E. J., & Marcy, J. F. (1952). Rep. investig. US bur. mines no. 4904.
- Health and Safety Laboratory. (2002). A review of the state-of-the-art in gas explosion modelling. HSL/2002/02. UK.
- Kosinski, P. and Hoffmann, A.C. (2006). An investigation of the consequences of primary dust explosions in interconnected vessels.
- Libby, P.A., & Williams, F.A. (1994). *Turbulence reacting flows*. London: Academic Press.
- Lunn, G. A., P. Holbrow, Andrews, S. and Gummer, J. (1996). "Dust Explosions in Totally Enclosed Interconnected Vessel Systems." *Journal of Loss Prevention in the Process Industries* , 9(1), 45-58.

- Magnussen, B. F., & Hjertager, B. H. (1977). On mathematical modelling of turbulent combustion with special emphasis on soot formation and combustion. In 16th Symp. (int.l) on combustion (pp. 719-729). The Combustion Institute.
- Maremonti, M., Russo, G., Salzano, E., & Tufano, V. (1999). Numerical simulation of gas explosions in linked vessels. *Journal of Loss Prevention in the Process Industries*, 12, 189-194.
- Marinov, N. (1990). *Electrotechnology in Mining*. Elsevier, Amsterdam.
- Mercx, W. P. M. (1997). Extended modelling and experimental research into gas explosions. In ESREL, international conference on safety and reliability, Lisbon, Portugal.
- Molkov, V., Dobashi, R., Suzuki, M., & Hirano, T. (2000). Venting of deflagrations: hydrocarbon-air and hydrogen-air systems. *Journal of Loss Prevention in the Process Industries*, 13, 397-409.
- Morton, K. W., & Mayers, D. F. (1994). *Numerical solution of partial differential equations*. UK: Cambridge University Press.
- Phylaktaou, H. and G. E. Andrews (1993). "Gas Explosions in Linked Vessels." *Journal of Loss Prevention in the Process Industries* 6(1): 15-19.
- Popat, N. R., Catlin, C. A., Arntzen, B. J., Lindstedt, R. P., Hjertager, B. H., Solberg, T., et al. (1996). Investigations to improve and assess the accuracy of computational fluid dynamic based explosion models. *Journal of Hazardous Materials*, 45, 1-25.
- Rogstadkjernet, L. (2004). *Combustion of Gas in Closed, Interconnected Vessels: Pressure Piling*. Thesis, University of Bergen, Department of Physics and Technology.
- Singh, J. (1977). Ph.D. thesis, University of London, British Library Ref. No. D24652/78.
- Singh, J. (1994). Gas explosions in inter-connected vessels: pressure piling. *Transactions of the IChemE*, 72B, 220-228.
- Spalding, D. B. (1977). Development of the Eddy-break-up model of turbulent combustion. In 16th Symp. (int.l) on combustion (pp. 1657-1663). The Combustion Institute.
- Taylor, J.R. (1994). *Risk Analysis for Process Plant, Pipelines and Transport*. London: E & F N SPON.
- Versteeg, H. K. and Malalasekera, W. (2007). *An Introduction to Computational Fluid Dynamics*. England: PEARSON Prentice Hall.

Veynante, D., & Vervisch, L. (2002). Turbulent combustion modeling. *Progress in Energy and Combustion Sciences*, 28, 193-266.